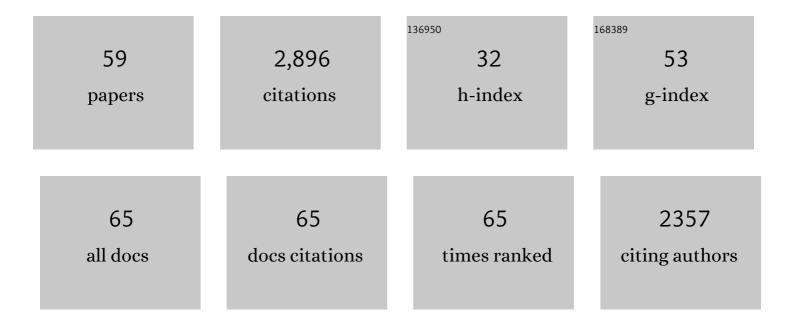
## Jeremy D Owens

List of Publications by Year in descending order

Source: https://exaly.com/author-pdf/2648449/publications.pdf

Version: 2024-02-01



#	Article	IF	CITATIONS
1	New evidence for a long Rhaetian from a Panthalassan succession (Wrangell Mountains, Alaska) and regional differences in carbon cycle perturbations at the Triassic-Jurassic transition. Earth and Planetary Science Letters, 2022, 577, 117262.	4.4	13
2	Iron and manganese shuttle has no effect on sedimentary thallium and vanadium isotope signatures in Black Sea sediments. Geochimica Et Cosmochimica Acta, 2022, 317, 218-233.	3.9	12
3	Geochemical Records Reveal Protracted and Differential Marine Redox Change Associated With Late Ordovician Climate and Mass Extinctions. AGU Advances, 2022, 3, .	5.4	17
4	Nanoscale trace-element zoning in pyrite framboids and implications for paleoproxy applications. Geology, 2022, 50, 736-740.	4.4	11
5	Vanadium isotope fractionation during hydrothermal sedimentation: Implications for the vanadium cycle in the oceans. Geochimica Et Cosmochimica Acta, 2022, 328, 168-184.	3.9	10
6	Biotic induction and microbial ecological dynamics of Oceanic Anoxic Event 2. Communications Earth & Environment, 2022, 3, .	6.8	5
7	Clobally distributed iridium layer preserved within the Chicxulub impact structure. Science Advances, 2021, 7, .	10.3	47
8	Behavior of the Mo, Tl, and U isotope systems during differentiation in the Kilauea Iki lava lake. Chemical Geology, 2021, 574, 120239.	3.3	19
9	Transient ocean oxygenation at end-Permian mass extinction onset shown by thallium isotopes. Nature Geoscience, 2021, 14, 678-683.	12.9	24
10	Thallium behavior during high-pressure metamorphism in the Western Alps, Europe. Chemical Geology, 2021, 579, 120349.	3.3	6
11	New constraints on mid-Proterozoic ocean redox from stable thallium isotope systematics of black shales. Geochimica Et Cosmochimica Acta, 2021, 315, 185-206.	3.9	6
12	A multi-proxy approach to constrain reducing conditions in the Baltic Basin during the late Silurian Lau carbon isotope excursion. Palaeogeography, Palaeoclimatology, Palaeoecology, 2021, 581, 110624.	2.3	9
13	Shifting modes of iron sulfidization at the onset of OAE-2 drive regional shifts in pyrite δ34S records. Chemical Geology, 2020, 553, 119808.	3.3	12
14	Geochemical signatures of redepositional environments: The Namibian continental margin. Marine Geology, 2020, 429, 106316.	2.1	7
15	Thallium isotope ratios in shales from South China and northwestern Canada suggest widespread O2 accumulation in marine bottom waters was an uncommon occurrence during the Ediacaran Period. Chemical Geology, 2020, 557, 119856.	3.3	25
16	Marine redox variability from Baltica during extinction events in the latest Ordovician–early Silurian. Palaeogeography, Palaeoclimatology, Palaeoecology, 2020, 554, 109792.	2.3	28
17	Integrated sedimentary, biotic, and paleoredox dynamics from multiple localities in southern Laurentia during the late Silurian (Ludfordian) extinction event. Palaeogeography, Palaeoclimatology, Palaeoecology, 2020, 553, 109799.	2.3	17
18	Sedimentary vanadium isotope signatures in low oxygen marine conditions. Geochimica Et Cosmochimica Acta, 2020, 284, 134-155.	3.9	26

JEREMY D OWENS

#	Article	IF	CITATIONS
19	Molybdenum isotope and trace metal signals in an iron-rich Mesoproterozoic ocean: A snapshot from the Vindhyan Basin, India. Precambrian Research, 2020, 343, 105718.	2.7	18
20	Constraining oceanic oxygenation during the Shuram excursion in South China using thallium isotopes. Geobiology, 2020, 18, 348-365.	2.4	37
21	Multiple negative molybdenum isotope excursions in the Doushantuo Formation (South China) fingerprint complex redox-related processes in the Ediacaran Nanhua Basin. Geochimica Et Cosmochimica Acta, 2019, 261, 191-209.	3.9	52
22	Linking the progressive expansion of reducing conditions to a stepwise mass extinction event in the late Silurian oceans. Geology, 2019, 47, 968-972.	4.4	40
23	Vanadium isotopic fractionation during the formation of marine ferromanganese crusts and nodules. Geochimica Et Cosmochimica Acta, 2019, 265, 371-385.	3.9	16
24	Cooling-driven oceanic anoxia across the Smithian/Spathian boundary (mid-Early Triassic). Earth-Science Reviews, 2019, 195, 133-146.	9.1	57
25	Geochemical evidence for expansion of marine euxinia during an early Silurian (Llandovery–Wenlock) Tj ETQq1	1 0.7843 4.4	14 rgBT /Ove
26	Fully oxygenated water columns over continental shelves before the Great Oxidation Event. Nature Geoscience, 2019, 12, 186-191.	12.9	95
27	Paired organic matter and pyrite Î'34S records reveal mechanisms of carbon, sulfur, and iron cycle disruption during Ocean Anoxic Event 2. Earth and Planetary Science Letters, 2019, 512, 27-38.	4.4	46
28	Absence of biomarker evidence for early eukaryotic life from the Mesoproterozoic Roper Group: Searching across a marine redox gradient in midâ€Proterozoic habitability. Geobiology, 2019, 17, 247-260.	2.4	39
29	Vanadium isotope composition of seawater. Geochimica Et Cosmochimica Acta, 2019, 244, 403-415.	3.9	32
30	Nucleosynthetic vanadium isotope heterogeneity of the early solar system recorded in chondritic meteorites. Earth and Planetary Science Letters, 2019, 505, 131-140.	4.4	23
31	Terrestrial sources as the primary delivery mechanism of mercury to the oceans across the Toarcian Oceanic Anoxic Event (Early Jurassic). Earth and Planetary Science Letters, 2019, 507, 62-72.	4.4	146
32	Rapid recovery of life at ground zero of the end-Cretaceous mass extinction. Nature, 2018, 558, 288-291.	27.8	123
33	Quantifying the missing sink for global organic carbon burial during a Cretaceous oceanic anoxic event. Earth and Planetary Science Letters, 2018, 499, 83-94.	4.4	52
34	The iron paleoredox proxies: A guide to the pitfalls, problems and proper practice. Numerische Mathematik, 2018, 318, 491-526.	1.4	174
35	An evaluation of sedimentary molybdenum and iron as proxies for pore fluid paleoredox conditions. Numerische Mathematik, 2018, 318, 527-556.	1.4	63
36	Tracking the rise of eukaryotes to ecological dominance with zinc isotopes. Geobiology, 2018, 16, 341-352.	2.4	65

JEREMY D OWENS

#	Article	IF	CITATIONS
37	Thallium isotopes reveal protracted anoxia during the Toarcian (Early Jurassic) associated with volcanism, carbon burial, and mass extinction. Proceedings of the National Academy of Sciences of the United States of America, 2018, 115, 6596-6601.	7.1	113
38	Organically bound iodine as a bottom-water redox proxy: Preliminary validation and application. Chemical Geology, 2017, 457, 95-106.	3.3	22
39	Constraining the rate of oceanic deoxygenation leading up to a Cretaceous Oceanic Anoxic Event (OAE-2: ~94 Ma). Science Advances, 2017, 3, e1701020.	10.3	87
40	Evidence for rapid weathering response to climatic warming during the Toarcian Oceanic Anoxic Event. Scientific Reports, 2017, 7, 5003.	3.3	102
41	Thallium-isotopic compositions of euxinic sediments as a proxy for global manganese-oxide burial. Geochimica Et Cosmochimica Acta, 2017, 213, 291-307.	3.9	65
42	Patterns of local and global redox variability during the Cenomanian–Turonian Boundary Event (Oceanic Anoxic Event 2) recorded in carbonates and shales from central Italy. Sedimentology, 2017, 64, 168-185.	3.1	45
43	Tracking along-arc sediment inputs to the Aleutian arc using thallium isotopes. Geochimica Et Cosmochimica Acta, 2016, 181, 217-237.	3.9	56
44	Sedimentary chromium isotopic compositions across the Cretaceous OAE2 at Demerara Rise Site 1258. Chemical Geology, 2016, 429, 85-92.	3.3	44
45	Empirical links between trace metal cycling and marine microbial ecology during a large perturbation to Earth's carbon cycle. Earth and Planetary Science Letters, 2016, 449, 407-417.	4.4	82
46	Analysis of high-precision vanadium isotope ratios by medium resolution MC-ICP-MS. Journal of Analytical Atomic Spectrometry, 2016, 31, 531-536.	3.0	31
47	Upper ocean oxygenation dynamics from I/Ca ratios during the Cenomanianâ€Turonian OAE 2. Paleoceanography, 2015, 30, 510-526.	3.0	60
48	Dynamic changes in sulfate sulfur isotopes preceding the Ediacaran Shuram Excursion. Geochimica Et Cosmochimica Acta, 2015, 170, 204-224.	3.9	36
49	Iron and manganese speciation and cycling in glacially influenced high-latitude fjord sediments (West) Tj ETQq1 Cosmochimica Acta, 2014, 141, 628-655.	1 0.78431 3.9	4 rgBT /Ov∘ 88
50	Upper Albian OAE 1d event in the Chihuahua Trough, New Mexico, U.S.A Cretaceous Research, 2013, 46, 136-150.	1.4	29
51	Sulfur isotopes track the global extent and dynamics of euxinia during Cretaceous Oceanic Anoxic Event 2. Proceedings of the National Academy of Sciences of the United States of America, 2013, 110, 18407-18412.	7.1	127
52	Sulfur record of rising and falling marine oxygen and sulfate levels during the Lomagundi event. Proceedings of the National Academy of Sciences of the United States of America, 2012, 109, 18300-18305.	7.1	174
53	Selenium as paleo-oceanographic proxy: A first assessment. Geochimica Et Cosmochimica Acta, 2012, 89, 302-317.	3.9	80
54	Iron isotope and trace metal records of iron cycling in the protoâ€North Atlantic during the Cenomanianâ€Turonian oceanic anoxic event (OAEâ€2). Paleoceanography, 2012, 27, .	3.0	56

JEREMY D OWENS

#	Article	IF	CITATIONS
55	Combing DNAzyme with single-walled carbon nanotubes for detection of Pb( <scp>ii</scp> ) in water. Analyst, The, 2011, 136, 764-768.	3.5	34
56	Trace metal enrichments in Lake Tanganyika sediments: Controls on trace metal burial in lacustrine systems. Geochimica Et Cosmochimica Acta, 2011, 75, 483-499.	3.9	18
57	Formation of syngenetic and early diagenetic iron minerals in the late Archean Mt. McRae Shale, Hamersley Basin, Australia: New insights on the patterns, controls and paleoenvironmental implications of authigenic mineral formation. Geochimica Et Cosmochimica Acta, 2011, 75, 1072-1087.	3.9	64
58	Joining forces: Combined biological and geochemical proxies reveal a complex but refined high-resolution palaeo-oxygen history in Devonian epeiric seas. Palaeogeography, Palaeoclimatology, Palaeoecology, 2011, 306, 134-146.	2.3	39
59	Extreme eolian delivery of reactive iron to late Paleozoic icehouse seas. Geology, 0, , G37226.1.	4.4	6